ROTATIONAL BANDS WITH $\pi g_{9/2}^{-2}$ STRUCTURE IN $Z \geq 50$, $N \sim 56$–65 Nuclei*

A.V. AFANASJEV[a,b,c], I. RAGNARSSON[a] AND J.M. SEARS[c]

[a]Department of Mathematical Physics, Lund Institute of Technology
Box 118, S-22100 Lund, Sweden
[b]Physik-Department der Technischen Universität München
D-85747 Garching, Germany
[c]Nuclear Research Center, Latvian Academy of Sciences
LV-2169, Salaspils, Miera str.31, Latvia
[d]Department of Physics, State University of New York at Stony Brook
Stony Brook, New York 11794, USA

(*Received December 18, 1995*)

The properties of rotational bands in the $A \sim 110$ ($Z \geq 50, N \sim$ 56–65) mass region are investigated within the configuration-dependent shell-correction approach with the cranked Nilsson potential. It is shown that in nuclei with $Z \geq 50, N \leq 60$, smooth terminating bands based on two proton holes in the $g_{9/2}$ subshell might be observed over a wide spin range up to termination. In the $N > 60$ nuclei, the terminating states of such bands reside well above the yrast line in calculations. The results of calculations are consistent with available experimental data.

PACS numbers: 21.60.Ev

1. Introduction

The rotational bands observed among the very neutron-deficient nuclei in the $A \sim 110$ ($Z \geq 50$, $N \sim 56$–65) mass region are interesting examples for the testing of theoretical models. These band structures show not only the highest rotational frequencies (up to $\hbar\omega \sim 1.5$ MeV) found in any mass region, facilitating a study of the properties of nuclei under extreme rotation, but also unusually low values of the dynamic moment of inertia $\mathcal{J}^{(2)}$ (1/3-1/2 of the rigid body value), indicating a large single-particle contribution to the total spin. Moreover, the lack of experimental evidence

* Presented at the "High Angular Momentum Phenomena" Workshop in honour of Zdzisław Szymański, Piaski, Poland, August 23–26, 1995.

for any quasiparticle alignment above a frequency of $\hbar\omega \sim 0.7$ MeV suggests that both proton and neutron pairing are significantly reduced in this mass region. Finally, there are some indications, for example in ^{109}Sb [1] and in ^{106}Sn [2], that these *terminating* bands can be observed over a wide spin range, from high-collectivity ($\varepsilon_2 \sim 0.24$–0.28) at low spin up to the terminating (pure particle-hole) state.

These indications are quite significant from both the theoretical and experimental points of view. In spite of the experimental observation of terminating bands or terminating states at high spin in the neighbourhood of ^{158}Er and also in the $A \sim 120$ mass region (among the I and Xe isotopes), the experimental data on terminating bands which are observed over several spin units up to termination are very limited. In most cases, the terminating bands observed in these mass regions represent examples of so-called *favoured termination*, in which the last spin units before termination are built at a low energy cost. Therefore, although the terminating states are yrast, with decreasing spin these terminating bands diverge very quickly away from the yrast line, placing severe limitations on their experimental observation over a wide spin range.

In the $A \sim 110$ ($Z \geq 50, N \sim 60$) mass region, the situation is exactly the opposite. The rotational bands observed over a wide spin range are typically associated with configurations based upon two proton holes in the $g_{9/2}$ orbitals and also intruder $h_{11/2}$ proton orbital(s) which are strongly deformation driving. As a result, their deformation at low spin ($\varepsilon_2 \sim 0.25$) is much larger than that for the yrast states ($\varepsilon_2 \sim 0.10 - 0.15$). Indeed, experimentally it has been possible to follow these bands down to low spin $I \sim 15\hbar$ where they are definitely non-yrast. At medium spins $I \sim 20$–$40\hbar$ these bands are favoured in energy in comparison with configurations based upon either one or three or more holes in the proton $g_{9/2}$ orbitals. As the energy cost for building the last spin units before termination is high, characteristic of *unfavoured termination*, it is generally reasonable to expect that the terminating states reside well above the yrast line. However, in some nuclei in the neighbourhood of ^{109}Sb, the rotational bands based on two proton holes in the $g_{9/2}$ subshell are strongly favoured in energy a few spin units before termination. The terminating state is thus still calculated to be yrast or close to yrast albeit the energy cost for building the last spin units is quite high. These bands are collective at low spin but show a continuous transition to pure particle-hole (terminating) states. As a result, we refer to them as *smooth terminating bands* [1].

A detailed investigation of the properties of smooth terminating bands in this mass region has been performed within the configuration-dependent shell-correction approach using the cranked Nilsson potential [3] with the parameter set from Ref. [4]. Pairing correlations are neglected in our calculations since they are expected to play a minor role at rotational frequencies above $\hbar\omega \sim 0.7$ MeV. The most important features of smooth terminating bands [1, 5] are summarized in Section 2. Although the rotational bands with $\pi g_{9/2}^{-2}$ structure in nuclei with $N > 60$ are yrast a few spin units before termination, their terminating states are expected to lie well above the yrast line. This conclusion will be demonstrated in Section 3, where the results of calculations for ^{111}Sn and ^{116}Te will be compared with recently observed rotational structures.

2. General properties of smooth terminating bands

There are several important features of smooth terminating bands in the $A \sim 110$ $(Z \geq 50, N \sim 60)$ mass region.

1. The high energy cost for building the last spin units in unfavoured terminating bands with $\pi g_{9/2}^{-2}$ structure arises primarily from *(i)* the difficulty to align the proton $g_{9/2}$ holes when they are surrounded by aligned particles; and *(ii)* the fact that the neutron $g_{7/2}/d_{5/2}$ subshells are essentially half-filled, *i.e.* the spin contributions from the last particles in these subshells is close to zero.
2. With increasing proton number above $Z = 53$, the collective rotational bands with no proton holes in the $g_{9/2}$ subshell become more favoured in energy at spins $I \sim 20 - 40\hbar$. In theoretical calculations these bands are yrast over a wide spin range up to termination and terminate in a rather favoured way.
3. With increasing neutron number above $N = 60$, the terminating states of rotational bands with two proton holes $(\pi g_{9/2}^{-2})$ are calculated to lie well above the yrast line. This is because the configurations of these bands involve more than seven neutrons from the $g_{7/2}$ / $d_{5/2}$ subshells, leading to negative contributions to the maximal spin of the bands from the eighth, ninth, ... neutrons in these subshells. As a result, a significant increase of the energy cost for building the last spin units before termination is calculated.
4. Approaching the terminating state, the contribution to $\mathcal{J}^{(2)}_{\mathrm{band}}$ from the alignment of valence particles becomes smaller while the contribution from the changing deformation increases. A typical situation $6 - 8\hbar$ before termination is that deformation changes contribute approximately one third of $\mathcal{J}^{(2)}_{\mathrm{band}}$.

3. Smooth terminating bands in $N > 60$ nuclei

A number of high-spin rotational bands have been observed recently in the $N > 60$ nuclei ^{111}Sn [6] and ^{116}Te [7]. Typical of unfavored termination, these bands manifest a decrease in the dynamic moment of inertia $\mathcal{J}^{(2)}$ down to 15 – $20\hbar^2$/MeV with increasing rotational frequency. The rotational structures in these two nuclei will be studied in this section in order to illustrate the third statement of Section 2 above.

An important difference between these two nuclei is connected with the position of the Fermi level in the proton subsystem. For Sn isotopes, it is possible to form energetically favourable configurations based on the proton $2p2h$ structure by putting two protons excited from the $g_{9/2}$ subshell into the $g_{7/2}$ / $d_{5/2}$ subshells. For Te isotopes, the favoured configurations with the same proton hole structure will include one or two protons in the intruder $h_{11/2}$ orbitals. Since intruder $h_{11/2}$ orbitals are strongly deformation driving, it is expected that the deformation of $\pi 4p2h$ rotational bands in ^{116}Te is greater than that of the $\pi 2p2h$ rotational bands in ^{111}Sn. In addition, the larger number of valence particles + valence holes outside of the closed core in ^{116}Te compared to ^{111}Sn leads to greater maximal spin for the ^{116}Te bands.

^{111}Sn. A decoupled band extending to a spin-parity of $(67/2^-)$ and a transition energy of (2070) keV was observed in ^{111}Sn [6]. This band was interpreted as the $\nu h_{11/2}$ valence orbital coupled to the deformed $[(\pi g_{7/2})^2 \otimes (\pi g_{9/2})^{-2}]$ ^{110}Sn core. This interpretation is supported by theoretical calculations shown in Fig. 1, where a reasonable agreement between experiment and theory for the configuration $[20,3]^-$ is observed at spins $I \geq 20\hbar$. The state which corresponds to the last state observed in the experiment, at $I = 33.5^-$ of configuration $[20,3]^-$, is calculated to be only $\sim$ 200 keV above the yrast line. Observation of this band to higher spin will apparently be quite difficult given that with increasing spin the assigned configuration $[20,3]^-$ diverges from the yrast line very quickly.

Band 1 in ^{116}Te. Several rotational bands have been observed recently in ^{116}Te [7], the most interesting of which is band 1, observed to the highest transition energy (2031 keV) and spin ($I = 42^+$). The configuration $[22,4]^+_a$ can be assigned for this band as illustrated in Fig. 2. Despite some differences in the slope between the $E - E_{RLD}$ curves for band 1 and configuration $[22,4]^+_a$ of Fig. 2, the calculations reproduce reasonably well the minimum of the experimental $E - E_{RLD}$ curve. Because pairing correlations are neglected, only a qualitative picture can be obtained for low spins $I < 30\hbar$. For example, the smoothly upsloping part of the experimental $E - E_{RLD}$ curve at spins $I = 14 - 26\hbar$ and the smooth crossing at $I = 26\hbar$ might be associated with a gentle crossing of the calculated $[22,4]^+_a$ and $[22,6]^+$ configurations, as suggested by Fig. 2.

Some remarks are needed with respect to the configuration assigned for band 1. With ten valence neutrons in the $g_{7/2}$ / $d_{5/2}$ orbitals, then the maximal spin which can be obtained within this configuration is equal to

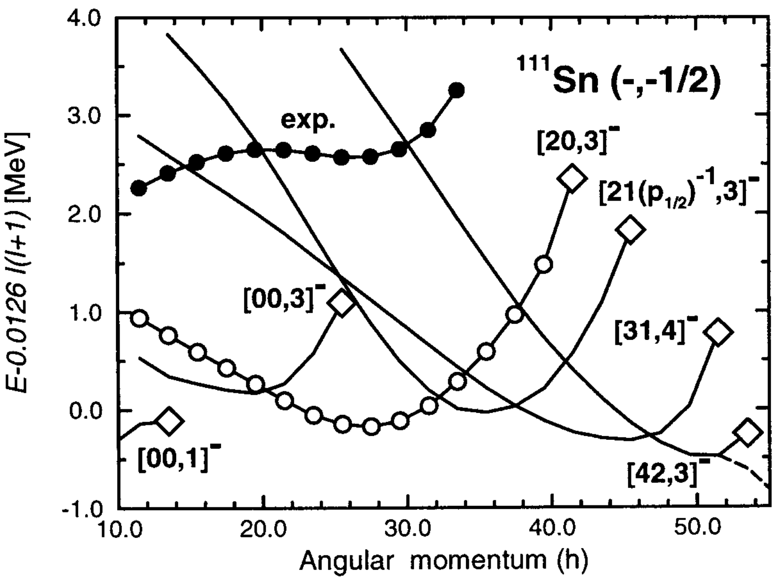

Fig. 1. Experimental band in ^{111}Sn and calculated yrast configurations with parity $\pi = -$ and signature $\alpha = -1/2$. The energies are given relative to a smooth liquid-drop expression $(\hbar^2/2\mathcal{J}_{rig})\, I(I+1)$, where the moment of inertia parameter $(\hbar^2/2\mathcal{J}_{rig}) =$ 0.0126 MeV. Aligned states (band terminations) are shown by open diamonds. Solid symbols are used for the experimental band. The calculated configuration which can be assigned to the observed band is shown by open symbols of the same type. The shorthand configuration labels in the figure indicate the number of proton holes in the $g_{9/2}$ orbital and the number of protons and neutrons in the $h_{11/2}$ orbitals as well as the parity of configuration by superscript. The detailed structure of the configurations relative to the spherical $^{100}_{50}\mathrm{Sn}_{50}$ core together with the calculated quadrupole deformation for the terminating states are given by the following, where $\pi[]_0$ indicates no contribution from the proton core.

$$[00,1]^- = \pi[]_0 \otimes \nu[(g_{7/2}\ d_{5/2})_8^{10}\ (h_{11/2})_{5.5}^1]_{13.5};\ \varepsilon_2^{BT} = 0.05$$

$$[00,3]^- = \pi[]_0 \otimes \nu[(g_{7/2}\ d_{5/2})_{12}^{8}\ (h_{11/2})_{13.5}^3]_{25.5};\ \varepsilon_2^{BT} = 0.06$$

$$[20,3]^- = \pi[(g_{7/2}\ d_{5/2})_6^{2}\ (g_{9/2})_8^{-2}]_{14} \otimes \nu[(g_{7/2}\ d_{5/2}\ d_{3/2})_{14}^{8}\ (h_{11/2})_{13.5}^3]_{27.5};\ \varepsilon_2^{BT} = 0.08$$

$$[21(p_{1/2})^{-1},3]^- = \pi[(g_{7/2}\ d_{5/2})_6^{2}\ (g_{9/2})_8^{-2}\ (h_{11/2})_{5.5}^1\ (p_{1/2})_{0.5}^{-1}]_{20} \otimes \nu[(g_{7/2}\ d_{5/2})_{12}^{8}\ (h_{11/2})_{13.5}^3]_{25.5};\ \varepsilon_2^{BT} = 0.176$$

$$[31,4]^- = \pi[(g_{7/2}\ d_{5/2})_6^{2}\ (g_{9/2})_{10.5}^{-3}\ (h_{11/2})_{5.5}^1]_{22} \otimes \nu[(g_{7/2}\ d_{5/2}\ d_{3/2})_{13.5}^{7}\ (h_{11/2})_{16}^4]_{29.5};\ \varepsilon_2^{BT} = 0.11$$

$$[42,3]^- = \pi[(g_{7/2}\ d_{5/2})_6^{2}\ (g_{9/2})_{12}^{-4}\ (h_{11/2})_{10}^2]_{28} \otimes \nu[(g_{7/2}\ d_{5/2})_{12}^{8}\ (h_{11/2})_{13.5}^3]_{25.5};\ \varepsilon_2^{BT} = 0.16.$$

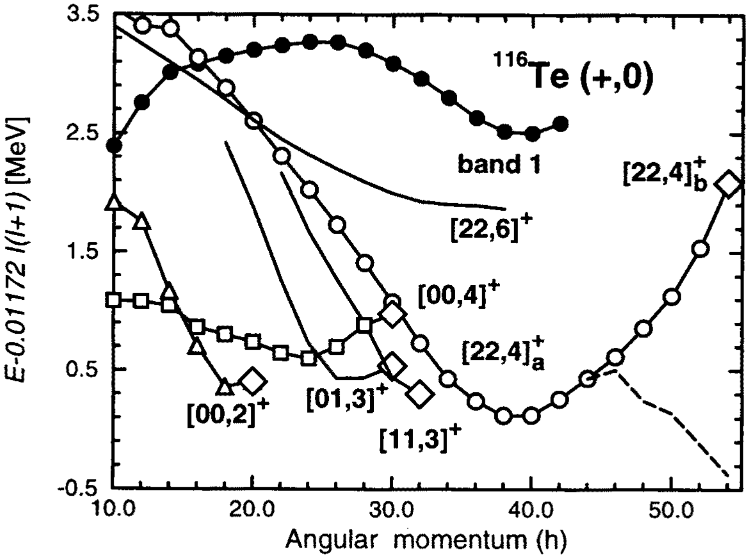

Fig. 2. Same as for Fig. 1, but for band 1 in ^{116}Te; only configurations with parity $\pi = +$ and signature $\alpha = 0$ are considered. The moment of inertia parameter used is $(\hbar^2/2\mathcal{J}_{rig}) = 0.01172$ MeV. The detailed structure of the configurations are as below.

$$[00,2]^+ = \pi[(g_{7/2}\ d_{5/2})^2_6]_6 \otimes \nu[(g_{7/2}\ d_{5/2})^{12}_4\ (h_{11/2})^2_{10}]_{14};\ \varepsilon_2^{BT} = 0.15$$

$$[01,3]^+ = \pi[(g_{7/2})^1_{3.5}\ (h_{11/2})^1_{5.5}]_9 \otimes \nu[(g_{7/2}\ d_{5/2})^{11}_{7.5}\ (h_{11/2})^3_{13.5}]_{21};\ \varepsilon_2^{BT} = 0.15$$

$$[00,4]^+ = \pi[(g_{7/2}\ d_{5/2})^2_6]_6 \otimes \nu[(g_{7/2}\ d_{5/2})^{10}_8\ (h_{11/2})^4_{16}]_{24};\ \varepsilon_2^{BT} = 0.14$$

$$[11,3]^+ = \pi[(g_{7/2}\ d_{5/2})^2_6\ (g_{9/2})^{-1}_{4.5}\ (h_{11/2})^1_{5.5}]_{16}$$
$$\otimes \nu[(g_{7/2}\ d_{5/2})^{11}_{2.5}\ (h_{11/2})^3_{13.5}]_{16};\ \varepsilon_2^{BT} = 0.20$$

$$[22,4]^+_a = \pi[(g_{7/2}\ d_{5/2})^2_6\ (g_{9/2})^{-2}_8\ (h_{11/2})^2_{10}]_{24}$$
$$\otimes \nu[(g_{7/2}\ d_{5/2})^{10}_{10}\ (h_{11/2})^4_{16}]_{26}$$

$$[22,4]^+_b = \pi[(g_{7/2}\ d_{5/2})^2_6\ (g_{9/2})^{-2}_8\ (h_{11/2})^2_{10}]_{24}$$
$$\otimes \nu[(g_{7/2}\ d_{5/2}\ d_{3/2}\ s_{1/2})^{10}_{14}\ (h_{11/2})^4_{16}]_{30};\ \varepsilon_2^{BT} = 0.10$$

$$[22,6]^+ = \pi[(g_{7/2}\ d_{5/2})^2\ (g_{9/2})^{-2}\ (h_{11/2})^2] \otimes \nu[(g_{7/2}\ d_{5/2})^8\ (h_{11/2})^6]$$

$I_{\max} = 50\hbar$ (conf. $[22,4]^+_a$, see caption of Fig. 2). However, in the calculated configuration, which should be labelled $[22,4]^+$, the requirement is instead that the ten valence protons are placed in the $g_{7/2}$ / $d_{5/2}$ / $d_{3/2}$ / $s_{1/2}$ orbitals giving a maximal spin of $I_{\max} = 54\hbar$. The interchange from configuration $[22,4]^+_a$ at low spin to the configuration $[22,4]^+_b$ at the termination can be seen from the calculated deformation changes. Below $I = 44\hbar$, the quadrupole deformation decreases and the γ-deformation increases smoothly with increasing spin. At this spin, however, the γ-deformation becomes significantly smaller than at $I = 42\hbar$, indicating that a change of occupied orbitals is taking place in the calculations. The position of the Fermi level in the neutron subsystem is such that with increasing rotational frequency, the $d_{3/2}$ / $s_{1/2}$ orbitals can become occupied instead of the ninth and tenth $g_{7/2}$ / $d_{5/2}$ orbitals. Indeed, at the calculated equilibrium deformation ($\varepsilon_2 = 0.209$, $\gamma = 15.7°$) and rotational frequency $\hbar\omega \sim 1.0$ MeV corresponding to the $I = 44^+$ state, the lowest $d_{3/2}$ / $s_{1/2}$ ($\alpha = -1/2$) Routhian (downsloping on the energy versus $\hbar\omega$ plot) is close in energy to the last occupied $g_{7/2}$ / $d_{5/2}$ ($\alpha = -1/2$) Routhian (upsloping), as demonstrated in Fig. 4 of Ref.[5]. As a result, the deformation change at $I = 44^+$ can be explained by promotion of one neutron from $g_{7/2}$ / $d_{5/2}$ ($\alpha = -1/2$) to $d_{3/2}$ / $s_{1/2}$ ($\alpha = -1/2$). Assuming that a second neutron is moved from the $g_{7/2}$ / $d_{5/2}$ ($\alpha = +1/2$) Routhian to the $d_{3/2}$ / $s_{1/2}$ ($\alpha = +1/2$) Routhian at a higher rotational frequency, the maximal spin becomes $I = 54\hbar$ (conf. $[22,4]_b^+$, caption of Fig. 2) which is equal to the spin of terminating state obtained in calculations. However, the calculations do not permit a unique definition of the spin at which the configuration $[22,4]_b^+$ becomes lowest. Since the orbitals belonging to the $g_{7/2}$, $d_{5/2}$, $d_{3/2}$ and $s_{1/2}$ subshells are treated in our calculations as one entity, it is not straightforward to treat configurations $[22,4]_a^+$ and $[22,4]_b^+$ separately or to define the proper position of the terminating state of configuration $[22,4]_a^+$ on the $E - E_{RLD}$ plot. However, the maximal spin for configuration $[22,4]_a^+$ is defined in a unique way and it is clear that its terminating $I = 50\hbar$ state lies above the $I = 50\hbar$ state of the $E - E_{RLD}$ curve corresponding to the combined $[22,4]_a^+$ and $[22,4]_b^+$ configurations of Fig. 2. As a result, the terminating $I = 50\hbar$ state is at least 1 MeV above the yrast line. A similar situation appears in calculations for configuration $[20,3]^-$ of ^{111}Sn: in this case, the calculated maximal spin suggests that one neutron is moved from the $g_{7/2}$ / $d_{5/2}$ ($\alpha = -1/2$) orbital into $d_{3/2}$ / $s_{1/2}$ ($\alpha = -1/2$) close to termination.

Because the configuration $[22,4]_a^+$ in ^{116}Te has two protons in the intruder $h_{11/2}$ orbitals, the calculated quadrupole deformation is significantly larger than that of the configuration assigned for the rotational band in ^{111}Sn. In addition, the calculations indicate positive triaxiality for this band over a wide spin range. For example, the calculated equilibrium deformations in ^{116}Te are ($\varepsilon_2 = 0.273, \gamma = 11.0°$), ($\varepsilon_2 = 0.259, \gamma = 13.3°$) and ($\varepsilon_2 = 0.231, \gamma = 21.9°$) at spin values of $20\hbar$, $30\hbar$ and $40\hbar$, respectively, which can be compared with the equilibrium deformations of configuration $[20,3]^-$ in ^{111}Sn of ($\varepsilon_2 = 0.227, \gamma = 3.1°$) and ($\varepsilon_2 = 0.197, \gamma = 13.4°$) at spins of $19.5\hbar$ and $29.5\hbar$, respectively.

A particularly interesting observation is that these rotational bands in ^{116}Te and ^{111}Sn are observed up to spin values which are close to the spin

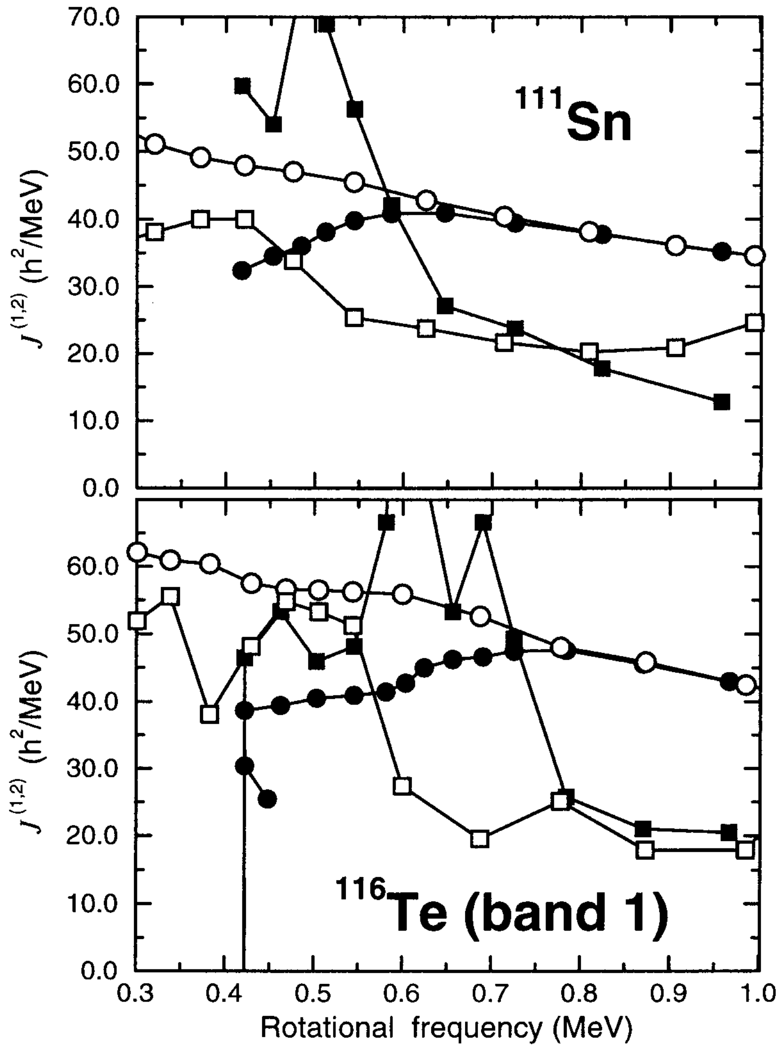

Fig. 3. Kinematic $\mathcal{J}^{(1)}$ and dynamic $\mathcal{J}^{(2)}$ moments of inertia for the rotational bands discussed in text. Solid symbols are used for experimental data and open symbols for calculated values. Circles indicate $\mathcal{J}^{(1)}$, squares $\mathcal{J}^{(2)}$.

values at which the calculated configurations assigned to them are crossed by other configurations, see Figs. 1 and 2. This suggests that the states with higher spin are non-yrast, consistent with the fact that they are not observed in experiment.

Smooth terminating bands reveal a fall off in the dynamic moment of inertia $\mathcal{J}^{(2)}$ with increasing rotational frequency. In most cases, this behavior is reproduced reasonably well within the configuration-dependent shell-correction approach (see Ref. [5]; the rotational structures in ^{111}Sn and ^{116}Te studied here are no exception. The kinematic $\mathcal{J}^{(1)}$ and dynamic $\mathcal{J}^{(2)}$ moments of inertia of the observed bands are consistent with calculations at rotational frequencies above $\hbar\omega \sim 0.7$ MeV where the pairing correlations are expected to play a minor role, as shown in Fig. 3.

4. Conclusion

The configuration-dependent shell correction approach with the cranked Nilsson potential has been employed for investigation of smooth terminating bands in the $A \sim 110$ mass region. Calculations suggest that in nuclei with $Z \sim 51$, $N \leq 60$, smooth terminating bands with two proton hole structure might be observed over a wide spin range up to termination. On the contrary, the terminating states of the bands in nuclei with $N > 60$ containing two proton holes in the $g_{9/2}$ subshell are calculated to be well above the yrast line, placing severe restrictions on the possibility to observe smooth terminating bands over a wide spin range up to termination. These calculations have been shown to be qualitatively consistent with available experimental data.

We are grateful for financial support from the Swedish Natural Science Research Council, the Nordic Council of Ministers (the Nordic Baltic Scholarship Scheme governed by the Swedish Institute) and the Royal Swedish Academy of Sciences. One of us (A.V.A.) also acknowledges support from the *Konferenz der Deutschen Akademien der Wissenschaften.*

REFERENCES

[1] I. Ragnarsson *et al.*, *Phys. Rev. Lett.* **74**, 3935 (1995).
[2] R. Wadsworth *et al.*, *Phys. Rev.* **C50**, 483 (1994).
[3] T. Bengtsson and I. Ragnarsson, *Nucl. Phys.* **A436**, 14 (1985).
[4] Jing-ye Zhang *et al.*, *Phys. Rev.* **C39**, 714 (1989).
[5] A.V. Afanasjev and I. Ragnarsson, *Nucl. Phys.* **A**, in press.
[6] D.R. LaFosse *et al.*, *Phys. Rev.* **C51**, R2876 (1995).
[7] J.M. Sears *et al.*, to be published.